

## Article

## Lipid Librations at the Interface with the Na,K-ATPase

Rita Guzzi,<sup>1</sup> Rosa Bartucci,<sup>1</sup> Mikael Esmann,<sup>2</sup> and Derek Marsh<sup>3,\*</sup><sup>1</sup>Department of Physics, Molecular Biophysics Laboratory and Consorzio Nazionale Interuniversitario per le Scienze Fisiche della Materia Unit, University of Calabria, Ponte P. Bucci, Rende, Italy; <sup>2</sup>Department of Biomedicine, Aarhus University, Aarhus, Denmark; and<sup>3</sup>Max-Planck-Institut für biophysikalische Chemie, Göttingen, Germany

**ABSTRACT** Transitions between conformational substates of membrane proteins can be driven by torsional librations in the protein that may be coupled to librational fluctuations of the lipid chains. Here, librational motion of spin-labeled lipid chains in membranous Na,K-ATPase is investigated by spin-echo electron paramagnetic resonance. Lipids at the protein interface are targeted by using negatively charged spin-labeled fatty acids that display selectivity of interaction with the Na,K-ATPase. Echo-detected electron paramagnetic resonance spectra from native membranes are corrected for the contribution from the bilayer regions of the membrane by using spectra from dispersions of the extracted membrane lipids. Lipid librations at the protein interface have a flat profile with chain position, whereas librational fluctuations of the bilayer lipids increase pronouncedly from C-9 onward, then flatten off toward the terminal methyl end of the chains. This difference is accounted for by increased torsional amplitude at the chain ends in bilayers, while the amplitude remains restricted throughout the chain at the protein interface with a limited lengthening in correlation time. The temperature dependence of chain librations at the protein interface strongly resembles that of the spin-labeled protein side chains, suggesting solvent-mediated transitions in the protein are driven by fluctuations in the lipid environment.

## INTRODUCTION

The function of integral membrane proteins, both transport systems and enzymes, depends on the surrounding lipid. The transmembrane sectors of the protein are interfaced with the lipid bilayer environment via a first shell of lipids with properties distinct from those of the bulk (1,2). Whereas the nanosecond rotational and conformational dynamics of the lipid chains interacting with transmembrane proteins are reasonably well studied (e.g., Marsh and Horváth (3)), little is known about their rapid librational motions such as are characterized for bilayer lipids by using pulse electron paramagnetic resonance (EPR) (4–7). It is worthwhile to note that these equilibrium librational fluctuations, which persist to lower temperatures, are able to drive functionally important motions (i.e., on-pathway conformational transitions) at physiological temperatures, as embodied by the fluctuation-dissipation theorem (8,9).

Here, we exploit the selectivity of interaction of ionized fatty acids with the Na,K-ATPase (10,11) to study librational chain dynamics at the lipid-protein interface in membranes with spin-echo EPR. Recently, such a strategy was used successfully to isolate the water penetration profile at the protein-lipid interface (12). The relaxation rates that are deduced here from the anisotropic decays of echo-detected spectra are determined by the product,  $\langle \alpha^2 \rangle \tau_c$ , of the mean-square librational amplitude,  $\langle \alpha^2 \rangle$ , and the librational correlation time,  $\tau_c$ , of the spin-labeled lipid chains.

The mean-square amplitude of the libration is obtained from the hyperfine anisotropy in the conventional spin-label EPR spectra. Combining this with the pulse-EPR data then gives the librational correlation time. Previously, we used similar spin-echo methods to characterize librational motions of the protein side chains (13). Therefore, we also seek to correlate these findings with the librational properties of the lipid environment. The librational characteristics of lipid chains at the protein interface differ significantly from those in the bilayer regions of the membrane. These librational motions of the interfacial lipid most likely couple to those that we detect in the protein and are responsible for driving transitions between on-pathway conformational substates (13,14).

## MATERIALS AND METHODS

## Materials

Stearic acids spin-labeled at the C-*n* position of the chain, *n*-SASL (*n*-(4,4-dimethylloxazolidine-*N*-oxyl) stearic acid), were synthesized as described in Marsh (15) and Marsh and Watts (16).

## Preparation of shark salt gland Na,K-ATPase

Na,K-ATPase from the rectal gland of *Squalus acanthias* was prepared as described previously in Skou and Esmann (17) but omitting the treatment with saponin. The Na,K-ATPase constituted typically ~70% of the total protein and the specific Na,K-ATPase activity was 1650  $\mu\text{mol}$  of ATP hydrolyzed per milligram of protein per hour (18). The enzyme is stable over the pH range 5.2–9.2 at low temperatures in the absence of salt (10); at higher temperatures, inactivation is inhibited by addition of salt (19).

Submitted January 14, 2015, and accepted for publication May 6, 2015.

\*Correspondence: [dmarsh@gwdg.de](mailto:dmarsh@gwdg.de)

Editor: Joseph Falke.

© 2015 by the Biophysical Society  
0006-3495/15/06/2825/8 \$2.00



Membrane lipids were extracted with  $\text{CHCl}_3/\text{MeOH}$  (2:1 v/v) as described in Bligh and Dyer (20).

### Spin-labeling of Na,K-ATPase membranes

Before addition of the spin-labeled lipids, the Na,K-ATPase membranes were pelleted by centrifugation at 220,000  $g$  for 60 min at 10°C. Pellets were taken up in a buffer containing 10 mM Tris and 1 mM CDTA at pH 8.9. Membranes were spin-labeled by addition of 5  $\mu\text{L}$  of concentrated  $n$ -SASL solution in EtOH to 0.5 mL of membrane suspension (10 mg protein/mL) giving spin-label/protein ratios (w/w) of 1:100 or 1:50. After incubation for 150 min at 14°C, the membranes were pelleted by centrifugation at 220,000  $g$  for 60 min at 14°C. The pellets were then transferred to 3-mm quartz EPR tubes and stored at  $-18^\circ\text{C}$ .

### Spin-labeling of extracted lipid membranes

Extracted lipids in  $\text{CHCl}_3/\text{MeOH}$  (2:1 v/v) were codissolved with 0.5 mol % of  $n$ -SASL in chloroform. The solvent was evaporated by placing the sample first in a stream of dry nitrogen and then under vacuum overnight. The dried lipids were finally dispersed at a concentration of 1 mg/mL in buffer at pH 9 (or in the same buffer as used for the Na,K-ATPase membrane preparation) by periodically vortexing and mixing at 45°C. The hydrated lipid bilayers were transferred to a standard 3-mm quartz EPR tube, concentrated by pelleting in a benchtop centrifuge and stored at  $-18^\circ\text{C}$  until use.

### EPR spectroscopy

Pulse-EPR data were collected on an ELEXSYS E580 9-GHz Fourier transform FT-EPR spectrometer (Bruker, Karlsruhe, Germany) equipped with a MD5 dielectric resonator and a CF 935P cryostat (Oxford Instruments, Abingdon, Oxfordshire, UK).

Partially relaxed two-pulse ( $\pi/2$ - $\tau$ - $\pi$ - $\tau$ -echo) echo-detected EPR spectra were obtained by recording the integrated spin-echo signal at fixed interpulse delay  $\tau$ , while sweeping the magnetic field,  $B$ . The window for the integration was 160 ns. The microwave pulse widths were 32 and 64 ns, with the microwave power adjusted to provide  $\pi/2$  and  $\pi$ -pulses, respectively. The original echo-detected (ED) spectra,  $ED_T(2\tau, B)$ , were corrected for instantaneous spin diffusion by normalizing with respect to those recorded at 77 K, where no molecular motion is expected. The corrected spectra,  $ED_T^{\text{corr}}(2\tau, B)$ , recorded at temperature  $T$  are plotted as a function of magnetic field,  $B$ , according to Erilov et al. (6),

$$ED_T^{\text{corr}}(2\tau, B) = ED_T(2\tau, B) \frac{ED_{77\text{K}}(2\tau_0, B)}{ED_{77\text{K}}(2\tau, B)}, \quad (1)$$

where  $\tau_0$  is the shortest value of  $\tau$  for which ED-spectra were obtained. Relaxation rates,  $W(B, \tau_1, \tau_2)$ , were determined from the ratio of corrected ED-spectra recorded at two different values,  $\tau_1$  and  $\tau_2$ , of the interpulse delay by using the relation (5)

$$W(B, \tau_1, \tau_2) = \ln \left[ \frac{ED(2\tau_1, B)}{ED(2\tau_2, B)} \right] \cdot \frac{1}{2(\tau_2 - \tau_1)}, \quad (2)$$

where  $ED(2\tau, B)$  is the ED-spectral line height at field position  $B$ . These relaxation rates are averaged over the time interval from  $\tau_1$  to  $\tau_2$ , and are characterized by the maximum values,  $W_L$  and  $W_H$ , determined in the low- and high-field regions, respectively, of the ED-spectra. Calibration of the  $W_L$  and  $W_H$  relaxation rates in terms of the amplitude-correlation time product,  $\langle \alpha^2 \rangle \tau_c$ , of rotational motion from low-amplitude librations is taken from the results of spectral simulations (5,6,21). Here,  $\alpha$  is the angular amplitude,  $\tau_c$  is the correlation time, and angular brackets indicate an average over the librational motion.

The intrinsic ED-spectrum of the lipid-protein interface,  $ED_b(2\tau, B)$ , is obtained from the experimental ED-spectra of native membranes and extracted lipids,  $ED_m(2\tau, B)$  and  $ED_f(2\tau, B)$ , respectively. The spectrum from the membrane is the weighted average of those from the bilayer regions of the membrane and the protein interface, i.e.,

$$ED_m = f_b ED_b + (1 - f_b) ED_f,$$

where  $f_b$  is the fraction of lipids at the protein interface, and the spectrum from the lipid-protein interface is, therefore,

$$ED_b(2\tau, B) = \frac{ED_m(2\tau, B) - ED_f(2\tau, B)}{f_b} + ED_f(2\tau, B), \quad (3)$$

where  $f_b$  is obtained from spectral subtractions with the conventional EPR spectra (22).

Conventional continuous-wave (CW) EPR spectra were recorded on an ESP-300 9-GHz spectrometer (Bruker, Karlsruhe, Germany) using 100-kHz field modulation; the spectrometer was equipped with an ER 4111VT temperature controller (Bruker).

## RESULTS

### ED EPR spectra

Fig. 1 shows the partially relaxed two-pulse, ED EPR spectra of positional isomers of spin-labeled stearic acid,  $n$ -SASL, in native Na,K-ATPase membranes (*left-hand side*) and in bilayers of the extracted membrane lipids (*right-hand side*). The spectra are recorded at 180 K and are given for increasing values of the echo delay time  $\tau$ . The dependence of the corrected ED-lineshapes on the  $\tau$ -delay reveals preferential relaxation in the intermediate spectral regions at low and high fields, which is characteristic of rapid, small-amplitude torsional librations (23,24). The corresponding relaxation spectra, as defined by Eq. 2, were evaluated for pairs of delay times,  $\tau_1$  and  $\tau_2$ .  $W$ -relaxation spectra evaluated for different pairs of  $\tau_1$  and  $\tau_2$  coincide to within the noise level, showing that the relaxation is close to exponential. This is consistent with the so-called isotropic model for librational dynamics, in which uncorrelated librational motions take place simultaneously about the nitroxide  $x$ -,  $y$ -, and  $z$  axes, but not with those for uniaxial libration (5).

Fig. 2 shows the temperature dependence of the  $W$ -relaxation rate for 5-SASL and 14-SASL in Na,K-membranes (*top panel*) and in bilayers of the extracted lipids (*middle panel*). The  $W$ -relaxation rate is calculated from the maximum intensity ratios ( $W_L$  and  $W_H$ ) in the low- and high-field regions, respectively (see Erilov et al. (5)). The temperature profiles of  $W_L$  (*open symbols*) and  $W_H$  (*solid symbols*) are very similar, in each case showing consistency between the low- and high-field regions of the ED-spectra. The two profiles are related by a numerical factor that reflects the different intrinsic sensitivities to angular motion of the high-field and low-field spectral regions. For native membranes, the relaxation rates are very similar at

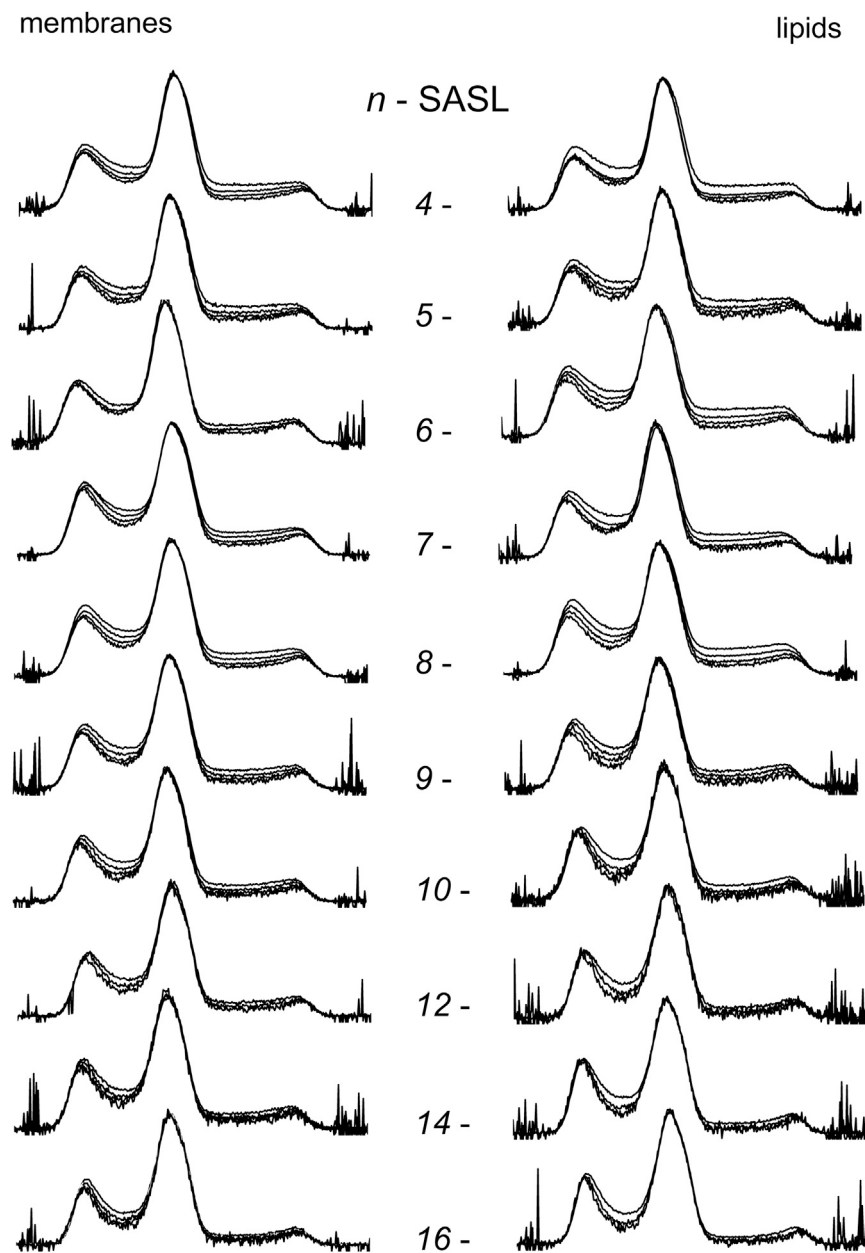


FIGURE 1 Echo-detected spectra of spin-labeled stearic acid (*n*-SASL) as a function of echo delay time,  $\tau$ , in native Na,K-ATPase membranes from *Squalus acanthias* (left column) and in bilayers of the extracted membrane lipids (right column), at pH 9 and  $T = 180$  K. The spectral line heights (*ED*) decrease with increasing  $\tau$ , which has the values: 168, 297, 424, and 527 ns. The position, *n*, of spin-labeling in the fatty acid chain of *n*-SASL is indicated on the figure. Total scan width = 10 mT.

the two positions of chain labeling (5-SASL and 14-SASL), whereas in the lipid bilayers they are very different. In particular, the relaxation rate increases more rapidly at lower temperatures for 14-SASL than for 5-SASL, and then flattens off before increasing again in the region of greatest increase for 5-SASL.

By using Eq. 3 in combination with Eq. 2, it is possible to determine the *W*-relaxation rates for the lipids at the protein interface. Data from lipid bilayers are combined with those from native membranes to give the values in the bottom panel of Fig. 2. The value of  $f_b = 0.43$  for ionized stearic acid at pH 9, which is needed to make this correction, is obtained from conventional CW EPR studies of lipid-protein

interactions (10). This pH is well above the  $pK_a$  of membrane-bound stearic acid (25,26).

### Librational dynamics

As already stated, the *W*-relaxation rate is determined by the product of the mean-square torsional amplitude  $\langle \alpha^2 \rangle$ , and the librational correlation time,  $\tau_c$  (5). Fig. 3 shows the temperature dependence of the librational amplitude-correlation time product,  $\langle \alpha^2 \rangle \tau_c$ , for 5-SASL and 14-SASL at the protein-lipid interface and in the lipid bilayer regions of Na,K-ATPase membranes. These values are obtained from the measurements of  $W_L$  that are given in Fig. 2, by using

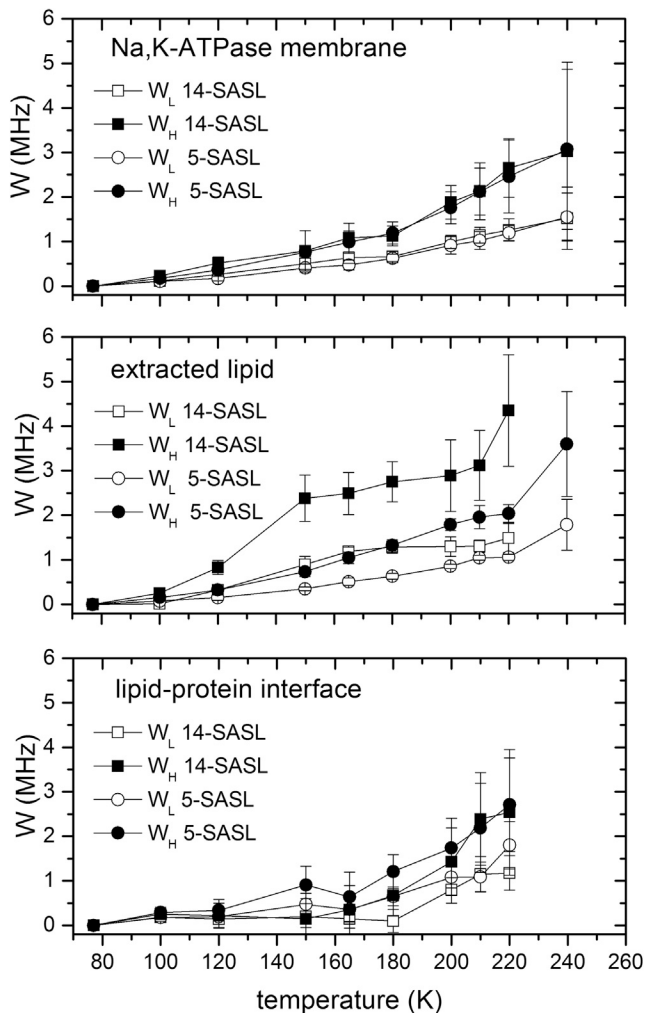


FIGURE 2 Temperature dependence of the relaxation rates,  $W$ , obtained from the ED-spectra of 5-SASL (circles) and 14-SASL (squares) in membranes from Na,K-ATPase (top) and the extracted lipids (middle). (Open and solid symbols) Relaxation rates for the low-field ( $W_L$ ) and high-field ( $W_H$ ) diagnostic regions, respectively. (Bottom, circles and squares) Values for 5-SASL and 14-SASL, respectively, at the protein lipid interface (obtained with Eq. 3).

conversion factors relating  $\langle \alpha^2 \rangle \tau_c$  to  $W_L$  of  $1.41$  and  $1.05 \times 10^{17} \text{ rad}^{-2} \text{ s}^{-2}$ , for 5-SASL and 14-SASL, respectively. This calibration was established previously for phosphatidylcholine spin-labeled in the *sn*-2 chain by using spectral simulations with the isotropic librational model (5,27). Unlike the situation in the bilayer regions of the membrane, the librational amplitude-correlation time product for lipids that interface directly with the intramembrane sector of the protein is very similar at the top (5-SASL) and bottom (14-SASL) of the chain.

### Hyperfine splittings and librational amplitudes

The upper panel of Fig. 4 shows the temperature dependences of the outer hyperfine splitting,  $2\langle A_{zz} \rangle$ , for the

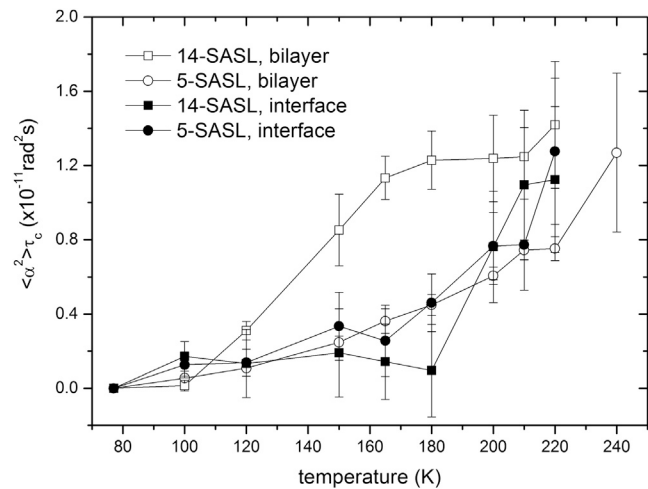


FIGURE 3 Temperature dependence of the amplitude-correlation product,  $\langle \alpha^2 \rangle \tau_c$ , for the librational motion of 5-SASL (circles) and 14-SASL (squares) at the protein-lipid interface (solid symbols) and in the lipid-bilayer regions (open symbols) of Na,K-ATPase membranes. Values are deduced from the  $W$ -relaxation rates in Fig. 2.

CW-EPR spectra from 5-SASL and 14-SASL in native Na,K-ATPase membranes and in bilayers of the extracted lipids. Initially, at low temperatures, the effective hyperfine splittings are approximately constant. Under these conditions, the hyperfine splittings correspond to their rigid-limit values,  $2A_{zz}$ , which depend mostly on the polarity of the spin-label environment (see, e.g., Marsh (28) and Kurad et al. (29)). This is comparable in membranes and lipid bilayers, at both positions of chain labeling.

Above 230–240 K, the values of  $2\langle A_{zz} \rangle$  decrease steeply with increasing temperature, as a result of progressive motional narrowing by rapid, small-amplitude torsional librations (30). For 14-SASL, toward the methyl end of the chain, the decrease of  $2\langle A_{zz} \rangle$  in this dynamic regime is greater for bilayers than it is for membranes. However, for 5-SASL, further up the chain, the two are similar. In both environments, the decrease at any given temperature is greater for 14-SASL than for 5-SASL, just as for the  $W$ -relaxation parameter (see Fig. 2 for comparison).

The lower panel of Fig. 4 shows the temperature dependence of the mean-square amplitude,  $\langle \alpha^2 \rangle$ , of the librational motion at the two positions of chain labeling for  $n$ -SASL in Na,K-ATPase membranes and bilayers of the extracted lipids. These values are derived from the motionally averaged hyperfine splittings, according to Bartucci et al. (27) and Van et al. (30),

$$\langle \alpha^2 \rangle = \frac{A_{zz} - \langle A_{zz} \rangle}{A_{zz} - A_{xx}}, \quad (4)$$

where the angular brackets indicate a motionally averaged hyperfine tensor (of principal elements  $A_{xx}$ ,  $A_{yy}$ , and  $A_{zz}$ ). The temperature dependences parallel (inversely) those of the motionally averaged hyperfine splittings in the upper



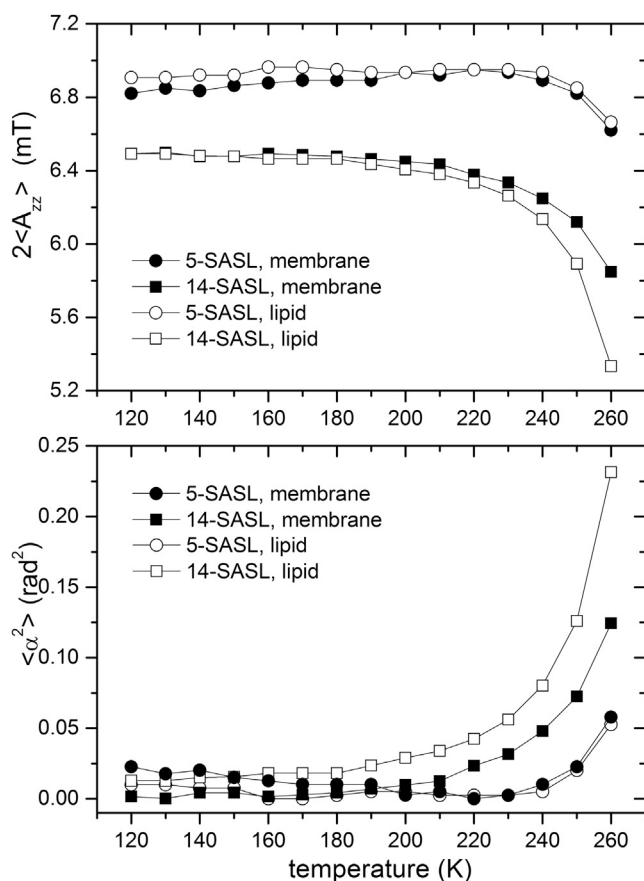


FIGURE 4 (Upper panel) Temperature dependence of the outer hyperfine splitting,  $2\langle A_{zz} \rangle$ , in the conventional EPR spectra of 5-SASL (circles) and 14-SASL (squares) in membranes from Na,K-ATPase (solid symbols) and the extracted lipids (open symbols). (Lower panel) Corresponding values of the mean-square librational amplitude,  $\langle \alpha^2 \rangle$  (see Eq. 4).

panel of the figure. The maximum values of  $\langle \alpha^2 \rangle$  recorded in Fig. 4 (at 260 K) correspond to root-mean-square amplitudes of  $\sim 5^\circ$  for 5-SASL, and  $12^\circ$  and  $16^\circ$  for 14-SASL in membranes and lipids, respectively. This justifies the small-amplitude approximation that is used in Eq. 4 (30).

### Librational correlation times

Fig. 5 shows the rotational correlation time,  $\tau_c$ , for the librational motion of 5-SASL and 14-SASL at the protein-lipid interface and in the lipid-bilayer regions of Na,K-ATPase membranes, at various temperatures. Determinations of the amplitude-correlation time product,  $\langle \alpha^2 \rangle \tau_c$ , from Fig. 3 are combined with the amplitude (i.e.,  $\langle \alpha^2 \rangle$ ) measurements that are given in Fig. 4 to obtain these values for  $\tau_c$ . Evaluations are possible only at temperatures of 200 K and higher, for which  $\langle \alpha^2 \rangle$  is nonzero. It is not feasible to correct the values of  $\langle \alpha^2 \rangle$  from membranes in the way that was done for the  $W$ -relaxation rate, because determination of the former relies on spectral splittings, not on intensities. For this reason it was assumed that values of  $\langle A_{zz} \rangle$  from

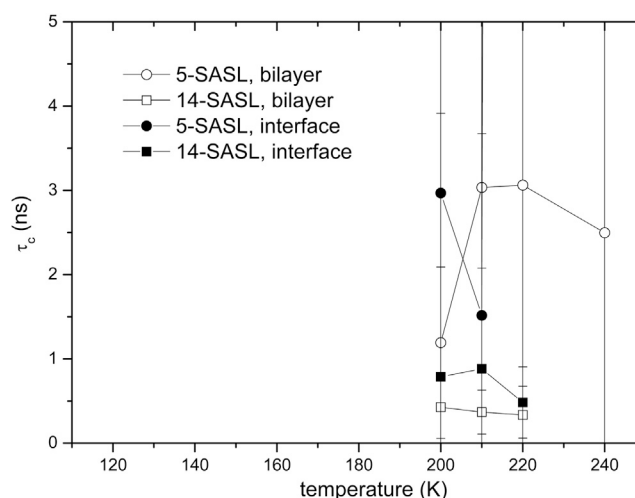


FIGURE 5 Librational correlation times,  $\tau_c$ , of 5-SASL (circles) and 14-SASL (squares) at the protein-lipid interface (solid symbols) and in the lipid-bilayer regions (open symbols) of Na,K-ATPase membranes. Values are deduced from the data of Figs. 3 and 4. Uncertainties become large at the higher temperatures (see text and Fig. 3).

the unresolved overlapping components in the membrane spectra were a suitable approximation to obtain  $\langle \alpha^2 \rangle$  for the lipid-protein interface. Consequently, these latter values are an upper estimate. The librational correlation times are longer at the 5-position of the lipid chain than at the 14-position, both in the bilayer regions of the membrane and at the protein interface. Data at 200 K, and for 14-SASL, suggest that lipid librational motions are slowed down somewhat by interaction with the protein. Beyond 200 K, the error bars become too large. These uncertainties arise because echo intensities are progressively weaker at the higher temperatures (see Fig. 3).

### Transmembrane profile

The upper panel of Fig. 6 shows the dependence on spin-label position,  $n$ , in the fatty acid chain of the  $W$ -relaxation rates for fully ionized  $n$ -SASL in membranes and in bilayers of the extracted lipids at 180 K. Reference to Fig. 2 shows that at this temperature the difference between 5-SASL and 14-SASL is largest. Both  $W_L$ - and  $W_H$ -rates exhibit consistent profiles, with a much more marked positional dependence for the extracted lipids than for the membranes. The ED-spectra from the lipids are used to correct those of the membranes, according to Eq. 3, to give the ED-spectra of the lipid/protein interface, as was done for the bottom panel of Fig. 2. The lower panel shows the resulting values of the amplitude-correlation time product,  $\langle \alpha^2 \rangle \tau_c$ , for the chain librations at the lipid/protein interface and in the bilayer regions of the membranes. These values are deduced from the  $W$ -relaxation rates as was described for Fig. 3. The profile in lipid bilayers shows an approximately constant amplitude-correlation time product up to C-9 of the chain,

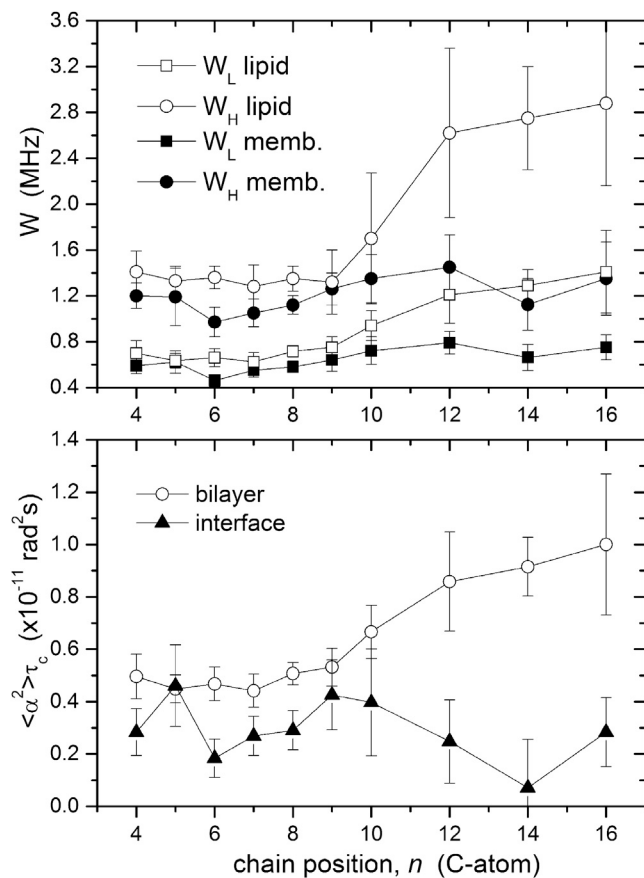


FIGURE 6 Positional profile,  $n$ , of  $W$ -relaxation rates,  $W_L$  and  $W_H$  (upper panel) of  $n$ -SASL in Na,K-ATPase membranes (solid symbols) and in bilayers of the extracted lipids (open symbols) at pH 9 and  $T = 180$  K. (Lower panel) Profile of the amplitude-correlation product,  $\langle \alpha^2 \rangle \tau_c$ , for the librational motion of chains in lipid bilayers (open symbols) and at the lipid/protein interface (solid symbols).

followed by a pronounced increase from C-10 onwards to the terminal methyl. This transbilayer profile resembles that found previously for phospholipid membranes containing 50 mol % of cholesterol (5). The values of  $\langle \alpha^2 \rangle \tau_c$  for the chains at the lipid/protein interface, on the other hand, are lower than those in the bilayer regions, and show no pronounced trend with position, although local inhomogeneities cannot be excluded.

## DISCUSSION

Conventional, continuous-wave EPR of natural and reconstituted membranes, including the Na,K-ATPase, shows that the lipids at the interface with integral membrane proteins are restricted in mobility on the nanosecond timescale, relative to those in fluid lipid bilayers (3,11,31). On a longer timescale, lipids at the protein interface exchange with fluid bilayer lipids, having residence times that depend on affinity for the protein and lie in the microsecond range (32–34). Typical turnover times for the overall and partial reactions

of the Na,K-ATPase are much longer than this (18,35). Consequently, the lipid-protein interface can be considered to be at exchange equilibrium during the enzymatic cycle, and it is the dynamic configuration of the interfacial lipids that modulates function. Here, we have concentrated on the librational motions of the spin-labeled lipid chains that can be studied by spin-echo EPR. The profile of the amplitude-correlation time product,  $\langle \alpha^2 \rangle \tau_c$ , at the protein interface differs considerably from that in bilayer membranes of the lipids alone (see Fig. 6).

In contrast to the lipid bilayer, where the librational amplitude-correlation time product is larger toward the end of the chain, with a transition in the region of C10–C12 (see also Erilov et al. (5)), the profile is essentially flat for lipid chains at the protein interface. Here,  $\langle \alpha^2 \rangle \tau_c$  remains at a relatively low level, comparable to that at the top of the chain in the bilayer lipids. Separating  $\langle \alpha^2 \rangle \tau_c$  into its amplitude and correlation time components reveals that differences in the transmembrane profile are attributable mostly to a larger amplitude toward the chain methyl ends in the bilayer. In the Na,K-ATPase membrane,  $\langle \alpha^2 \rangle$  is similar at the 5- and 14-C positions, whereas the angular amplitude is higher in the lipid bilayers and greater at the 14-C position than at the 5-position of the chain. The librational correlation time at the 14-C position is longer at the interface than in the bilayer, but comparable in both environments at the 5-position, where it is considerably longer than at the 14-position.

Librational motions of the Na,K-ATPase protein were characterized previously by using spin-labels covalently attached to cysteine residues (13). We can compare the librational fluctuations of the lipids with those of the protein by means of the temperature dependence of the  $W$ -relaxation rate and the librational averaged outer hyperfine splitting,  $2\langle A_{zz} \rangle$ . As seen from Figs. 2 and 4, these differ considerably between the bilayer lipids and lipids at the protein interface. Comparison with data from the spin-labeled protein (see Fig. 7) shows that the temperature dependence of the  $W$ -rates for interfacial lipids corresponds closely with that for spin-labeled –SH groups, but not with that for the bilayer lipids. Also, the onset of librational averaging of  $\langle A_{zz} \rangle$  occurs at a lower temperature for the bilayer lipids than for the lipid-protein interface and the protein-attached spin-labels (see Fig. 7).

Librational motions of lipids at the protein interface are coupled both to those of the protein and to those of the bilayer lipids. They provide a channel for dynamic communication between the two. Possibly, protein librations are slaved to those of the membrane environment via the interfacial lipids, as suggested previously for solvent-mediated interactions with soluble proteins (36,37). Interestingly, the solvent-dependent temperature profiles of the  $W$ -parameter for spin-labeled aqueous hemoglobin (38) differ qualitatively from those of the lipid-embedded Na,K-ATPase, which also differ somewhat from spin-labeled aqueous serum albumin (21). Such librational motions in

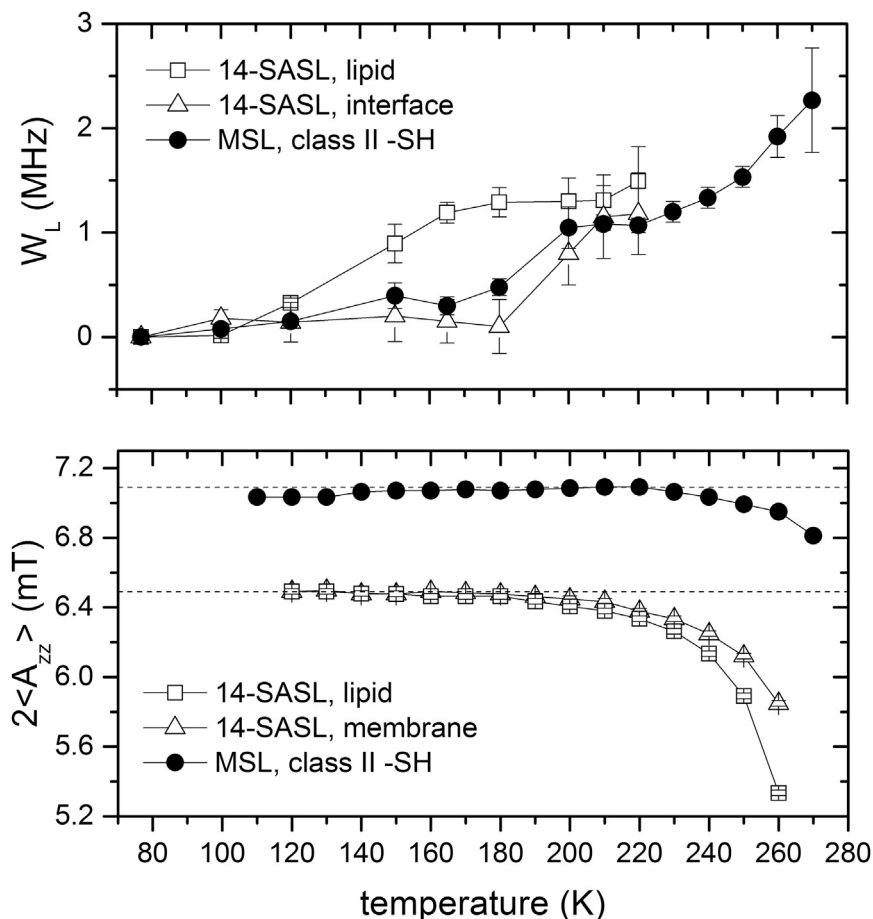


FIGURE 7 Temperature dependences of the  $W_L$ -relaxation rate (upper panel), and outer hyperfine splitting  $2\langle A_{zz} \rangle$  (lower panel), for membranous Na,K-ATPase covalently spin-labeled on Class II -SH groups (see Guzzi et al. (13)). (Solid circles) Data for the spin-labeled protein. (Open symbols) Corresponding data for spin-labeled lipid (14-SASL) in lipid bilayers (squares) and at the lipid-protein interface (triangles) (see Figs. 2 and 4).

the Na,K-ATPase could drive transitions between the different conformational substates that are frozen at lower temperatures but contribute to pathways between the principal enzymatic intermediates at higher temperatures (13).

## AUTHOR CONTRIBUTIONS

All authors designed research; R.G. and R.B. performed research and analyzed data; and M.E. contributed biochemical expertise and preparations.

## REFERENCES

1. Marsh, D. 2010. Electron spin resonance in membrane research: protein-lipid interactions from challenging beginnings to state of the art. *Eur. Biophys. J.* 39:513–525.
2. Marsh, D. 2008. Protein modulation of lipids, and vice-versa, in membranes. *Biochim. Biophys. Acta.* 1778:1545–1575.
3. Marsh, D., and L. I. Horváth. 1998. Structure, dynamics and composition of the lipid-protein interface. Perspectives from spin-labeling. *Biochim. Biophys. Acta.* 1376:267–296.
4. Bartucci, R., R. Guzzi, ..., L. Sportelli. 2003. Chain dynamics in the low-temperature phases of lipid membranes by electron spin-echo spectroscopy. *J. Magn. Reson.* 162:371–379.
5. Erilov, D. A., R. Bartucci, ..., L. Sportelli. 2004. Librational motion of spin-labeled lipids in high-cholesterol containing membranes from echo-detected EPR spectra. *Biophys. J.* 87:3873–3881.
6. Erilov, D. A., R. Bartucci, ..., L. Sportelli. 2004. Echo-detected electron paramagnetic resonance spectra of spin-labeled lipids in membrane model systems. *J. Phys. Chem. B.* 108:4501–4507.
7. Surovtsev, N. V., N. V. Ivanisenko, ..., S. A. Dzuba. 2012. Low-temperature dynamical and structural properties of saturated and monounsaturated phospholipid bilayers revealed by Raman and spin-label EPR spectroscopy. *J. Phys. Chem. B.* 116:8139–8144.
8. Kubo, R. 1966. Fluctuation-dissipation theorem. *Rep. Prog. Phys.* 29:255–284.
9. Frauenfelder, H., and E. Gratton. 1986. Protein dynamics and hydration. *Methods Enzymol.* 127:207–216.
10. Esmann, M., and D. Marsh. 1985. Spin-label studies on the origin of the specificity of lipid-protein interactions in  $\text{Na}^+/\text{K}^+$ -ATPase membranes from *Squalus acanthias*. *Biochemistry.* 24:3572–3578.
11. Esmann, M., and D. Marsh. 2006. Lipid-protein interactions with the Na,K-ATPase. *Chem. Phys. Lipids.* 141:94–104.
12. Bartucci, R., R. Guzzi, ..., D. Marsh. 2014. Water penetration profile at the protein-lipid interface in Na,K-ATPase membranes. *Biophys. J.* 107:1375–1382.
13. Guzzi, R., R. Bartucci, ..., D. Marsh. 2009. Conformational heterogeneity and spin-labeled -SH groups: pulsed EPR of Na,K-ATPase. *Biochemistry.* 48:8343–8354.
14. Guzzi, R., R. Bartucci, and D. Marsh. 2014. Heterogeneity of protein substates visualized by spin-label EPR. *Biophys. J.* 106:716–722.
15. Marsh, D. 2008. Electron spin resonance in membrane research: protein-lipid interactions. *Methods.* 46:83–96.

16. Marsh, D., and A. Watts. 1982. Spin-labeling and lipid-protein interactions in membranes. In *Lipid-Protein Interactions, Vol. 2* P. C. Jost, and O. H. Griffith, editors. Wiley-Interscience, New York, pp. 53–126.
17. Skou, J. C., and M. Esmann. 1979. Preparation of membrane-bound and of solubilized ( $\text{Na}^+ + \text{K}^+$ )-ATPase from rectal glands of *Squalus acanthias*. The effect of preparative procedures on purity, specific and molar activity. *Biochim. Biophys. Acta.* 567:436–444.
18. Esmann, M. 1988. ATPase and phosphatase activity of  $\text{Na}^+, \text{K}^+$ -ATPase: molar and specific activity, protein determination. *Methods Enzymol.* 156:105–115.
19. Fodor, E., N. U. Fedosova, ..., M. Esmann. 2008. Stabilization of  $\text{Na}, \text{K}$ -ATPase by ionic interactions. *Biochim. Biophys. Acta.* 1778:835–843.
20. Bligh, E. G., and W. J. Dyer. 1959. A rapid method of total lipid extraction and purification. *Can. J. Biochem. Physiol.* 37:911–917.
21. De Simone, F., R. Guzzi, ..., R. Bartucci. 2007. Electron spin-echo studies of spin-labelled lipid membranes and free fatty acids interacting with human serum albumin. *Biochim. Biophys. Acta.* 1768:1541–1549.
22. Esmann, M., A. Watts, and D. Marsh. 1985. Spin-label studies of lipid-protein interactions in ( $\text{Na}^+, \text{K}^+$ )-ATPase membranes from rectal glands of *Squalus acanthias*. *Biochemistry.* 24:1386–1393.
23. Dzuba, S. A., Yu. D. Tsvetkov, and A. G. Maryasov. 1992. Echo-detected EPR spectra of nitroxides in organic glasses: model of orientational molecular motions near equilibrium position. *Chem. Phys. Lett.* 188:217–222.
24. Dzuba, S. A. 1996. Librational motion of guest spin probe molecules in glassy media. *Phys. Lett. A.* 213:77–84.
25. Miyazaki, J., K. Hideg, and D. Marsh. 1992. Interfacial ionization and partitioning of membrane-bound local anesthetics. *Biochim. Biophys. Acta.* 1103:62–68.
26. Sankaram, M. B., P. J. Brophy, ..., D. Marsh. 1990. Fatty acid pH titration and the selectivity of interaction with extrinsic proteins in dimyristoylphosphatidylglycerol dispersions. Spin label ESR studies. *Biochim. Biophys. Acta.* 1021:63–69.
27. Bartucci, R., R. Guzzi, ..., D. Marsh. 2008. Backbone dynamics of alamethicin bound to lipid membranes: spin-echo electron paramagnetic resonance of TOAC-spin labels. *Biophys. J.* 94:2698–2705.
28. Marsh, D. 2002. Polarity contributions to hyperfine splittings of hydrogen-bonded nitroxides—the microenvironment of spin labels. *J. Magn. Reson.* 157:114–118.
29. Kurad, D., G. Jeschke, and D. Marsh. 2003. Lipid membrane polarity profiles by high-field EPR. *Biophys. J.* 85:1025–1033.
30. Van, S. P., G. B. Birrell, and O. H. Griffith. 1974. Rapid anisotropic motion of spin labels. Models for motion averaging of the ESR parameters. *J. Magn. Reson.* 15:444–459.
31. Marsh, D., and T. Páli. 2004. The protein-lipid interface: perspectives from magnetic resonance and crystal structures. *Biochim. Biophys. Acta.* 1666:118–141.
32. Horváth, L. I., P. J. Brophy, and D. Marsh. 1993. Exchange rates at the lipid-protein interface of the myelin proteolipid protein determined by saturation transfer electron spin resonance and continuous wave saturation studies. *Biophys. J.* 64:622–631.
33. Horváth, L. I., P. J. Brophy, and D. Marsh. 1988. Exchange rates at the lipid-protein interface of myelin proteolipid protein studied by spin-label electron spin resonance. *Biochemistry.* 27:46–52.
34. Arora, A., M. Esmann, and D. Marsh. 1999. Microsecond motions of the lipids associated with trypsinized  $\text{Na}, \text{K}$ -ATPase membranes. Progressive saturation spin-label electron spin resonance studies. *Biochemistry.* 38:10084–10091.
35. Esmann, M., and J. C. Skou. 1988. Temperature-dependencies of various catalytic activities of membrane-bound  $\text{Na}^+/\text{K}^+$ -ATPase from ox brain, ox kidney and shark rectal gland and of C12E8-solubilized shark  $\text{Na}^+/\text{K}^+$ -ATPase. *Biochim. Biophys. Acta.* 944:344–350.
36. Frauenfelder, H., P. W. Fenimore, ..., B. H. McMahon. 2006. Protein folding is slaved to solvent motions. *Proc. Natl. Acad. Sci. USA.* 103:15469–15472.
37. Young, R. D., and P. W. Fenimore. 2011. Coupling of protein and environment fluctuations. *Biochim. Biophys. Acta.* 1814:916–921.
38. Scarpelli, F., R. Bartucci, ..., R. Guzzi. 2011. Solvent effect on librational dynamics of spin-labeled hemoglobin by ED- and CW-EPR. *Eur. Biophys. J.* 40:273–279.